

Research on Parameter Identification Method for Hydrostatic Guideway Joint Based on Frequency Response Function

Pengfei Wu^{a,b}, Feng Gao^b

^a Key Lab. of NC Machine Tools and Integrated Manufacturing Equipment of the Education Ministry & Key Lab of Manufacturing Equipment of Shaanxi Province, Xi'an University of Technology, Xi'an 710048, China

^b Sichuan college of Architectural Technology, Mechanical Engineering, Deyang 618000, Sichuan, China
 pengfeiwu28391@126.com

Research the application of hydrostatic guideway in the field of modern ultra-precision machining technology. Optimize and analyze the structure design of machinable hydrostatic guideway with CCOS to obtain an optimized design scheme. Demonstrate the design scheme in this paper is effective through the stimulation of bearing deformation of slide plate before and after the structural improvement. According to the results of stimulation research, it can be confirmed that the optimization design of hydrostatic guideway is a practicable improvement plan.

1. Introduction

Hydrostatic guide way, a kind of research technology that is highly valued in modern ultra-precision machining technology, belongs to new technology in the field of core components of modern hydrostatic guideway, which still has insufficient popularity. However, after comparing with traditional ultra-precision grinding and manual grinding, it can be found that, ultra-precision grinding has higher precision requirement and processing cost, manual grinding has lower processing efficiency and yield as well as long process cycle, while the hydrostatic guideway not only has advantages including higher efficiency and accuracy, but also can avoid the disadvantages. In order to better control the hydrostatic guideway technology, the modern related fields will adopt frequency response function to control the hydrostatic guideway technology. Thus, this paper researches the parameter identification method for hydrostatic guideway technology by mainly focusing on the frequency response function.

This paper researches the structure and core parameters design of hydrostatic guideway. According to the comparative analysis on three typical hydrostatic guideway force models at home and abroad, it proposes a hydrostatic guideway structure with grind ability, designs the core parameters of hydrostatic guideway based on the hydrostatic support theory, and further provides a new idea for the design of precision hydrostatic guideway. After that, it researches the hydraulic oil film flow rate, pressure distribution and other features under simplified conditions by using Ansys/Fluen finite element analysis software through simulating and researching the physical characteristics of hydraulic oil film of hydrostatic guideway.

2. Literature review

The paper focuses on the identification of elastostatic properties of an industrial serial robot mounted on a rail. It proposes an identification procedure in order to find the optimal robot configuration to minimize the impact of measurement errors on the identification accuracy of the stiffness parameters. An experimental setup is designed to perform the identification of all stiffness parameters under industrial conditions. The proposed identification procedure is easy to use and takes little time (Guerin et al., 2014). Hydrostatic lubricated vertical guideway is commonly used as a form of rail head bearing lubrication in CNC vertical lathe lubricated bearing (Zhang et al., 2014). A three-dimensional finite element analysis of a rail/wheel contact is conducted on the rail joint section of track and dynamic load is applied to develop an estimate respective stresses at the section. The aim of this work is to adjust the position and size of the contact elements (spheres) and the model parameters in order to obtain both, a predicted motion provided by forward dynamics as faithful as possible to

the captured motion and a resultant foot–ground wrench (obtained through the foot–ground contact model) as close as possible to the measured foot–ground reactions. The results show that the obtained motion is really similar to the captured one and, moreover, the vertical force and the moments in the horizontal plane are in agreement with the experimental measurements. However, the bristle friction model used for tangential forces provides lower level of agreement with the experimental data.

These models should be accurately calculating the 3D stress response in the contact region. The reason for this study is to investigate possible changes in rail and wheel contact design in order to improve the performance of the rail track (Katheriya, 2014). In particular, its super linear convergence is proved under a second-order condition. The convergence of the solution to the approximating problem as the smoothing parameter goes to zero is shown. A strategy for adaptively selecting the regularization parameter based on a balancing principle is suggested (Clason and Jin, 2012). The rectangular pad is widely used in the hydrostatic guide rail, but hydrostatic guide rail in conditions for the emergence of the partial load or deformation factors, makes the hydrostatic guide rail in tilted state of bearing capacity of oil pad has a certain influence. This micro element method to establish hydrostatic guide rail are based on the actual working conditions of Reynolds equation, and then based on the finite difference method (Zhao and Li, 2016). A new parameter identification method for a three-dimensional foot–ground contact model is presented. The model is used to reproduce the relationship between the contact forces and the relative foot–ground displacements and velocities. The parameters of the contact model are estimated using the optimization method known as covariance matrix adaptation evolution strategy.

A universal dynamic model of fixed joints is built through considering the relative motion between the sub-structures of the fixed joints and the coupling among various degrees of freedom (Mao et al., 2010).

We propose a unified computational approach that involves solving a dynamic optimization problem, whose cost function measures the discrepancy between predicted and observed system output, to determine optimal values for the unknown quantities. Our main contribution is to show that the partial derivatives of this cost function can be computed by solving a set of auxiliary time-delay systems (Chai et al., 2013). Abstract Parameter identification methods are used to find optimal parameter values to fit models to measured data. The single integral method was defined as a simple and robust parameter identification method (Docherty, 2012). An extended Kalman filter is implemented as a controller to compute a forward dynamic analysis of the foot motion using body segment parameters and the ankle joint wrench as input data. The identified model parameters were used to generate the respective battery models for both healthy and degraded batteries. These models were then validated by comparing the model output voltage with the experimental output voltage for the stated operating conditions. The identified Li-Ion battery electrochemical model parameters are within reasonable accuracy as evidenced by the experimental validation results. Calibration results of a single FEA showed the repeatability of the pressure actuated bending angles, and the proposed dynamic model can precisely reproduce the deformation behavior of the FEA. Grasping experiments showed that the proposed dynamic model can predict the grasping forces, which was validated by a separate experiment of grasping force measurement. The presented methods can be extended to model other soft robots.

3. Method

3.1 Optimization and analysis of hydrostatic guideway structure design with machinability of CCOS

Compared with open hydrostatic guideway, the closed one has more sophisticated structure and bigger processing difficulty. The traditional guideway components machining method is grinding and manual grinding etc. In general, for the grinding of precision parts, the motion accuracy and feed resolution of grinding machine precision parts is often required to be an order of magnitude higher than the shape and dimensional accuracy of parts and it is also required to strictly control the clamping precision of parts. Therefore, the application of precision grinding method to control the shape and dimensional accuracy of guideway parts requires more processing cost. Manual grinding is an old processing method, and the machining accuracy is mainly guaranteed by the experience of grinding technician. In contrast, manual grinding has lower processing efficiency and yield.

The basic thought of computer controlled optical surfacing (referred to as CCOS) was firstly proposed by W.J.Rupp from Itek Company (USA) in 1970s. The basic principle is shown in Figure 1. Based on quantitative surface measurement data, it establishes a control model of machining process and uses the computer to control a small grinding head to grind or polish the machined parts. The motion of small grinding head includes the rotation motion around the rotation axis 1 with an angular velocity of ω_1 and revolution movement around the rotation axis 2 with an angular velocity of ω_2 . Furthermore, a pressure P is applied to the small grinding head when it is running. Finally, the residence time of small grinding head on the surface of work piece can be controlled through regulating the working speed of X and Y axis of machine, so as to precisely control the amount of material removal.

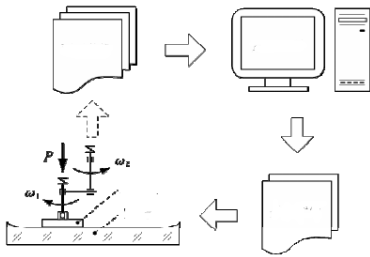


Figure 1: CCOS principle and flow diagram of processing plane

Fringe effect may be existed in CCOS machining process, which is caused by the relative pressure change when the polishing tool is moved to the edge of the work piece and the short residence time of the grinding disc in the edge area. In order to effectively control the “fringe effect”, technicians have done a lot of work and summarized some experiences, and one of the experiences was that, the leakage edge of the grinding disc is not more than 1/3 of the diameter of the grinding disc. For the purpose of achieving the desired surface precision of the processed parts, there must be enough space on the external edge of the machined surface to allow the disc to get out of the edge of the surface in order to control the "fringe effect".

As shown in Figure 2, the enlarged view on the left is the partial enlarged view of the contact area between the horizontal slider and base, and the base surface of contact area is a high-precision surface to be processed. It can be seen from the figure that, this plane is closely next to a vertical wall, if CCOS is used to machine such plane, the grinding disc will not be able to exit the plane due to the spatial interference of the vertical wall. Therefore, it is unable to use CCOS to machine the surface with high precision because of the structural design defects of original Nanoform-350 machine. In order to make the left and right hydrostatic bearing surfaces on the base work with CCOS technology, the space position of the bearing surface needs to be optimized and adjusted. The structure of optimized guideway is shown in Figure 3.

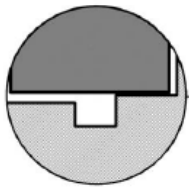


Figure 2: before improvement

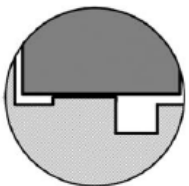


Figure 3: improved after improvement

3.2 Theoretical force analysis and optimization of hydrostatic guideway after the improvement of structure

Figure 4 shows the force analysis of hydrostatic guideway after the improvement of structure. First, the whole structure of guideway is divided into carriage and base. Providing the components in the hydraulic film formation area is subjected to uniform forces, the distribution of force from those two parts as shown as uniform arrows in the figure.

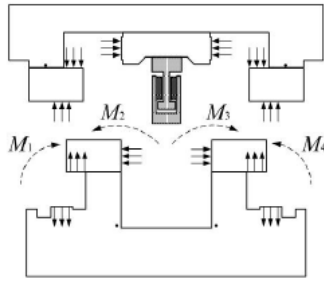


Figure 4: force analysis diagram of optimized hydrostatic guideway structure

Move all the forces on the base horizontally to the corresponding black origins in the figure (the black origin indicates the zero deformation position of supporting block if the ground of base and the surface of carriage worktable are fully fixed), then the base will be affected by the integrated effect of torque M_1 , M_2 , M_3 and M_4 other than the force passing through the origin as shown as the dotted arrow in the figure. It is revealed by the comparison that, although the position of hydrostatic supporting surface of the base displacements to the outside of base and further leads to the displacement of hydrostatic supporting force outside, such force will not cause any change of torque undertaken by the base, the deformation of base is mainly caused by the torsional deformation caused by the torque. Thus, the force deformation on the base after the structural improvement will not be changed.

Figure 5 and 6 show the carriage force analysis before and after the improvement. Providing the body of carriage is sufficiently rigid, it will not warp when subjected to an external load. Set the external load force to $2F$, and the load acts on the symmetrical center of the carriage. Under the above assumptions, the carriage will transmit the external load evenly to the supporting legs (the supporting legs will be deformed under the action of load) on both sides, and such supporting legs are connected with slider assembly. Assuming the supporting leg does not separate from the slider assembly surface under the action of external load, they will remain in contact all the time.

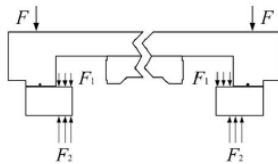


Figure 5: Pre improved force prototyping

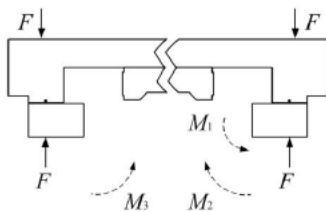


Figure 6: Improved equivalent stress

As shown in the figure, after the carriage is affected by the action of $2F$ external load, regardless of whether the guideway structure is improved or not, the single slider of guideway will be affected by the load of carriage, and the size of this load is F . After the carriage is subjected to an external load, it will generate a certain displacement in the direction of the load, and such displacement will result in changes in the film gap on both sides of slider, i.e., the upper hydraulic oil film support force is reduced to F_1 , while the lower hydraulic oil film support force is increased to F_2 , $F_2 - F_1 = F$.

Compare with the force before and after the structural improvement in Figure 5 and 6, the position of slider subject to the lower and upper hydraulic oil film support force after the structural improvement is changed, and

they are not on a line. An equivalent force diagram is obtained after the equivalently decomposing the force of slider in the figure.

The equivalent principle is as follows:

Make an equivalent subtraction of the upper and lower supporting force affected by the slider along the vertical direction, and the force affecting the slider upward along the vertical direction is equivalent to the F after subtraction. Moreover, this force still acts on the original position of the supporting force of the hydraulic oil film.

From the figure, it can be seen that, after the equivalence, the hydrostatic guideway before structural improvement only receives the action of vertical upward force F . This force is equivalently translated, so that it passes through the zero deformation point. Equivalently translate this force and make it pass through the zero deformation position point to produce a torque M_3 , which moves in counterclockwise direction, and the size equals to F multiples the force arm between it and the zero deformation position point. Except the vertical upward force F , the hydrostatic guideway is also affected by the torque M_1 works along the counterclockwise direction after the structural improvement. Similarly, equivalently translate the action force F and produce an equivalent torque M_2 , such torque works along the clockwise direction and opposite to M_1 . Compared with the hydrostatic guideway before the structural improvement, this force arm is short, so the value of torque is also relatively small.

4. Result and analysis

4.1 Stimulation of bearing deformation on the carriage before and after the structural improvement

In order to verify the conclusion of theoretic analysis above, a finite element stimulation analysis has been conducted for carriage, please find the results from Figure 7 and 8.

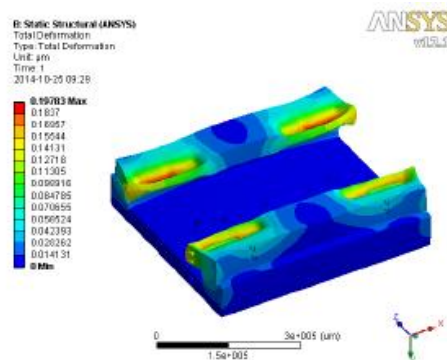


Figure 7: improved and optimized after carrying 2000N

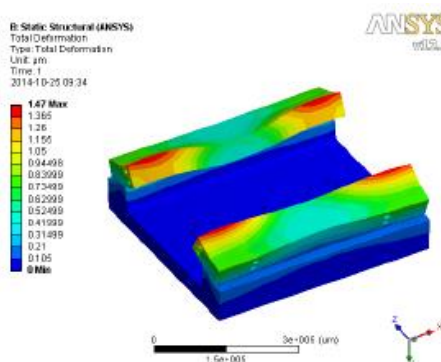


Figure 8: displacement is greater than optimal value carrying 2000N

According to the results, it can be found that, the torque M_1 is bigger than M_2 due to the continuous increase of displacement, and the slider is also affected by the action of integrated torque in the same direction as that of M_1 , which further lead to the torsional deformation of slider again. From the results, the torsional

deformation direction of slider is same as the theoretical analysis, and the maximum deformation is up to 1.47 μm , which is about 8 times than the extrusion deformation in the figure.

In summary, reasonable allocation of outward displacement for lower hydrostatic support oil film will not cause the change of force deformation on the base of guideway, but also can reduce the structural deformation of carriage. Therefore, on the basis of optimizing the CCOS machinability of the hydrostatic guide rail, this structural improvement program further improves the bearing performance of hydrostatic guideway, which is a practical and feasible improvement plan.

5. Conclusion

Firstly, this paper carries out the optimization and analysis on the structural design of hydrostatic guideway with CCOS machinability, and understands its disadvantages such as, sophisticated structure and big processing difficulty. Then it introduces and researches the CCOS, and obtains the material removal for precise control. Secondly, it gets the structural improvement plan through the theoretical force analysis and optimization of hydrostatic guideway after the structural improvement, and provides new ideas to improve the bearing performance of hydrostatic guideway. Finally, in order to verify the effectiveness of results, it conducts a stimulation experiment, and the results shows that the outward displacement of hydrostatic supporting oil film under reasonable allocation will not cause any change of force deformation on the base of guideway, but can reduce the structural deformation of carriage. Therefore, this structural improvement plan further improves the bearing performance of hydrostatic guideway based on the CCOS machinability of hydrostatic guideway, which is a practical and feasible improvement plan.

Reference

- Chai Q., Loxton R., Teo K.L., Yang C., 2013, A unified parameter identification method for nonlinear time-delay systems, *Journal of Industrial & Management Optimization*, 9(2), 471-486, DOI: 10.3934/jimo.2013.9.471
- Clason C., Jin B., 2012, A semismooth newton method for nonlinear parameter identification problems with impulsive noise, *Siam Journal on Imaging Sciences*, 5(2), 505-536, DOI: 10.1137/110826187
- Docherty P.D., Chase J.G., 2012, Characterisation of the iterative integral parameter identification method, *Medical & Biological Engineering & Computing*, 50(2), 127-134. DOI: 10.1007/s11517-011-0851-y
- Guerin D., Caro S., Garnier S., Girin A., 2014, Optimal measurement pose selection for joint stiffness identification of an industrial robot mounted on a rail. *Ieee/asme International Conference on Advanced Intelligent Mechatronics* (5), 1722-1727, DOI: 10.1109/aim.2014.6878332
- Katheriya P., 2014, An investigation of effects of axle load and train speed at rail joint using finite element method, 3(8), 41-47, DOI: 10.15623/ijret.2014.0308008
- Mao K., Li B., Wu J., Shao X., 2010, Stiffness influential factors-based dynamic modeling and its parameter identification method of fixed joints in machine tools, *International Journal of Machine Tools & Manufacture*, 50(2), 156-164, DOI: 10.1016/j.ijmachtools.2009.10.017
- Zhang Y.Q., Yu Z.Y., Li W.W., Yang X.D., Shao J.P., Yu X.D., 2014, Oil film flow-state analysis of hydrostatic vertical guideway of cnc vertical lathe rail head, *Key Engineering Materials*, 620, 110-115, DOI: 10.4028/www.scientific.net/kem.620.110
- Zhao Y., Li Y., 2016, Hydrostatic Guide Rail in Tilt State Oil Pad Bearing Performance Analysis, *International Conference on Computer Science and Mechanical Automation*, 322-325, DOI: 10.1109/csma.2015.71